

# ATF DEVELOPMENTS IN FALCON V1 AT PSI

C. COZZO, G. KHVOSTOV

*Laboratory for Reactor Physics and Thermal-Hydraulics  
Paul Scherrer Institut, Forschungsstrasse 111, 5232 Villigen, Switzerland*

## ABSTRACT

Accident tolerant fuels (ATF) are being developed to enhance the safety margin of commercial nuclear reactors while maintaining or improving economic efficiency of nuclear power; however the behavior of these materials has not been fully integrated in simulation tools yet. Internationally, a strong focus is put on the evolutionary concepts such as e.g. the use of  $U_3Si_2$  fuel with SiC cladding. A research version of the Falcon fuel behavior code has been developed at PSI as part of multi-physics assessment of ATF concepts. The first results are shown in this paper. The modelled properties are described and the results of calculation are verified. The performance of  $U_3Si_2/SiC$  is compared to that of  $UO_2/Zry-4$  for standard operational conditions in a PWR. The higher swelling rate of the uranium silicide is addressed by evaluating the effects of pellet growth on gap closure. While having a lower melting point, uranium silicide exhibits a high thermal conductivity that could counteract the lower thermal conductivity of SiC cladding.

## 1. Introduction

The station blackout (SBO) accidents at three of the Japanese Fukushima Dai-ichi reactors following the devastating 2011 earthquake and tsunami have sparked renewed interest in innovative fuel designs, so-called Accident Tolerant Fuels (ATFs, also called Advanced Technology Fuels), that would improve the performance and safety of current LWRs under situations ranging from operating conditions to design-basis accident and beyond-design-basis accident scenarios.

Among the envisioned ATF designs, SiC composite fuel cladding (SiC/SiC) is identified as one of the most promising technologies and this material is already being tested in several countries. While pure SiC fibres can exhibit a very high thermal conductivity, composite SiC cladding can, however, possess a transverse thermal conductivity lower than that of zircaloy, leading to higher fuel temperatures. This challenge can be overcome by the use of  $U_3Si_2$  as a candidate pellet material for ATFs, which exhibits much higher thermal conductivity than  $UO_2$ . The  $U_3Si_2/SiC$  concept (i.e. uranium silicide fuel with silicon carbide cladding) has been considered since several years [1]. This concept has been is currently subject to extensive simulation studies [2], [3]. This paper presents selected models for  $U_3Si_2$  fuel that have been implemented in a fuel performance code, along with the results of simulation for the  $U_3Si_2/SiC$  concept, as applied to base irradiation of the fuel rods.

## 2. Physical models

### 2.1 Reference fuel type

The study employs conventional uranium-dioxide fuel with a Zry-4 cladding as a reference case.

### 2.2 Silicon Carbide Cladding

SiC cladding models for a Duplex material have been originally implemented by EPRI in the fuel behaviour code Falcon [4], including the following SiC/SiC material properties: specific

heat, thermal conductivity, irradiation swelling, Young's modulus, yield stress, ultimate tensile stress and shear modulus. More specifically, the yield stress is calculated as follows [5]:

$$\sigma_{yield}[Pa] = 2.66 \cdot 10^4 \cdot T_{clad}[K] + 2.0 \cdot 10^8 \quad (1)$$

The differential thermal expansion coefficient and density were set to constants and the creep and oxidation are, at this stage, ignored and set to zero. It is understood that the cladding creep is a critical property and measurements have been currently performed at PSI to support modelling of this property.

Furthermore, PSI has developed a model for thermal conductivity, having reviewed literature data, and carried out steady-state measurements on pre-irradiated samples [6]. At this stage, a significant scatter in measured values makes it difficult to develop a new model. So far, it could be confidently concluded that thermal conductivity of SiC decreases with irradiation dose as the structure becomes more and more damaged. A thermal conductivity value of 4 W/m/K after reaching a saturation of the irradiation-induced degradation is globally recognized; therefore, conservatively, the thermal conductivity of SiC was set constant and equal to this value.

## 2.3 Uranium Silicide Fuel

### 2.3.1 Burnup Calculation

The burnup increment over a time step,  $\Delta t$ , is calculated with equation (2), where LHGR [W/m] is the average linear heat generation rate,  $\Delta t$  [s] the time increment,  $M_L$  [g<sub>v</sub>/m] the linear fuel mass density at a given axial position, and  $f_U$  [-] the weight fraction of uranium in the fuel (0.9273 for U<sub>3</sub>Si<sub>2</sub>).

$$\Delta Bu = \frac{LHGR \cdot \Delta t}{M_L \cdot f_U} \quad (2)$$

### 2.3.2 Physical Properties

As proposed by White [7], a constant coefficient of thermal expansion is calculated with equation (3):

$$\frac{\Delta L}{L} [-] = 16.1 \cdot 10^{-6} \cdot T[K] \quad (3)$$

The corrected correlation of White [8] for the thermal conductivity of unirradiated U<sub>3</sub>Si<sub>2</sub> is expressed in equation (4):

$$\lambda \left[ \frac{W}{m \cdot K} \right] = 0.0118 \cdot T[K] + 4.996 \quad (4)$$

It should be noted that, unlike for UO<sub>2</sub>, the thermal conductivity of U<sub>3</sub>Si<sub>2</sub> increases with temperature, which suggests, potentially, a better thermal behaviour of the ATF system.

In the same study, White proposed a correlation for the heat capacity of U<sub>3</sub>Si<sub>2</sub> in function of temperature, as shown in equation (5):

$$C_p \left[ \frac{J}{mol \cdot K} \right] = 0.02585 \cdot T[K] + 140.5 \quad (5)$$

Back in 1957 Kaufmann [9] estimated the melting point of U<sub>3</sub>Si<sub>2</sub> at ca. 1938 K. That value is still used nowadays, e.g. in [10]. 1938 K is set as melting point in Falcon.

The theoretical density (TD) of  $U_3Si_2$  is set to a value  $\rho [g/cm^3] = 12.16$  recommended in [11]. Westinghouse, together with INL, have produced  $U_3Si_2$  fuel pellets with as-fabricated porosity below 6 % [12].

### 2.3.3 Mechanical Properties

Carvajal-Nunez [13] reported a Young's modulus of  $U_3Si_2$  in the range 150-167 GPa. The constant value  $E = 155$  GPa is used in Falcon.

Taylor [14] carried out a study on the effect of density, in the range 90.2-97.7 % TD, on Poisson ratio. However, his measurements had a considerable scatter and no correlation could, at this stage, be derived. Nevertheless, the results currently used are in agreement with Taylor's measurement. Shimizu [15] later proposed the value of 0.17 for  $U_3Si_2$  with 92 % TD. For high-density material, White uses a value of 0.185. These values are used as boundaries to build the Poisson ratio model in Falcon, shown in equation (6):

$$v[-] = 3.2 \cdot 10^{-1} \cdot \frac{\rho}{\rho_{th}} - 1.2764 \cdot 10^{-1} \quad (6)$$

Metzger [2] has carried out an extensive study of  $U_3Si_2$  creep. Her models are however not included and fuel creep is not modelled in the current work – noting that it will be done in a later phase of the project.

### 2.3.4 Irradiation Behavior

Metzger [2] used an empirical expression for the swelling strain of  $U_3Si_2$  in function of the burnup expressed in FIMA ( equation (7) ). It is based on Finlay's analysis [16] of experimental results carried out with  $U_3Si_2$ -Al compounds [17].

$$\left(\frac{V}{V_0}\right) [\%] = 3.88008 \cdot Bu^2 + 0.79811 \cdot Bu \quad (7)$$

The equation is given in FIMA and Falcon calculates the swelling with MWd/kg<sub>U</sub>. Therefore, a conversion is required:  $100\%FIMA = 9.337 \cdot 10^2 MWd/kg_U$ .

In the absence of experimental data, it is assumed that the densification will be similar for  $U_3Si_2$  and  $UO_2$ . The ESCORE densification model of the Falcon code [18] is used in this study.

## 3. Simulation

### 3.1 Code

The simulations were carried out with the EPRI fuel performance code Falcon [18]. The code version is a development version based on Falcon 1.3.1.

Falcon is a state-of-the-art analysis code designed to calculate behaviour of a single LWR fuel rod under normal operation, operational power manoeuvres, and transients/postulated accidents. The code is built on a 2-dimensional finite element formulation of fully coupled time dependent thermal and mechanical modules. Full-length fuel rod analyses are performed using an axisymmetric R-Z (radial-axial) representation. The modelled fuel rod consists of two plugs at top and bottom locations, upper- and lower- gas plenums, fuel stack, gap elements and cladding element separating the fuel from the coolant. The rod was divided axially into 32 fuel elements, plus 1 upper- and 1 lower- plenum and plugs. Radially, the rod was modelled with 5 fuel element columns, 1 gap element and 5 cladding element columns.

Since PSI is part of the Falcon development team, the code has been modified in order to allow simulating  $U_3Si_2$  fuel. Scoping analysis for  $UO_2/SiC$  and  $U_3Si_2/Zr$  concepts, as intermediate steps, are performed in order to understand the impact of each material change in comparison to the reference  $UO_2/Zry$  case.

### 3.2 Operation Boundary Conditions

A representative rod for the peripheral channel of the Zion NPP, as described in the BEMUSE report [19] is studied. During the entire irradiation in the Zion core, the power shape used is the one provided in that document.

Since no Zion specific information is available, the one of a Swiss PWR (Pressurised Water Reactor) 5-cycle rod has been used as a reference and up-scaled to meet the BEMUSE final boundary conditions, as described in [20]. The assumed linear heat generation rate (LHGR) history is shown in Figure 1.

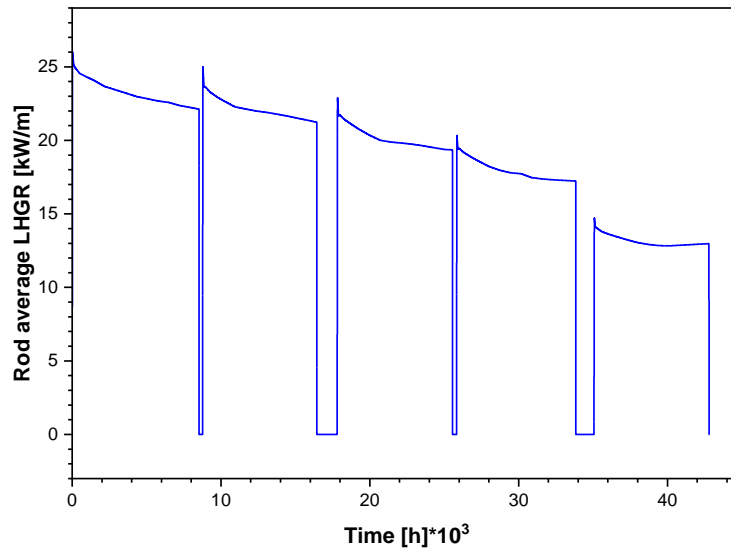


Figure 1: Average LHGR history of the PWR rod.

### 4. Results and discussion

The calculated burnup differs slightly for the two fuel-types considered (see Figure 2), therefore the results will be shown as function of irradiation time. The results at the end of irradiation are reported before the last shutdown, so that the fuel properties are shown as under the operating conditions.

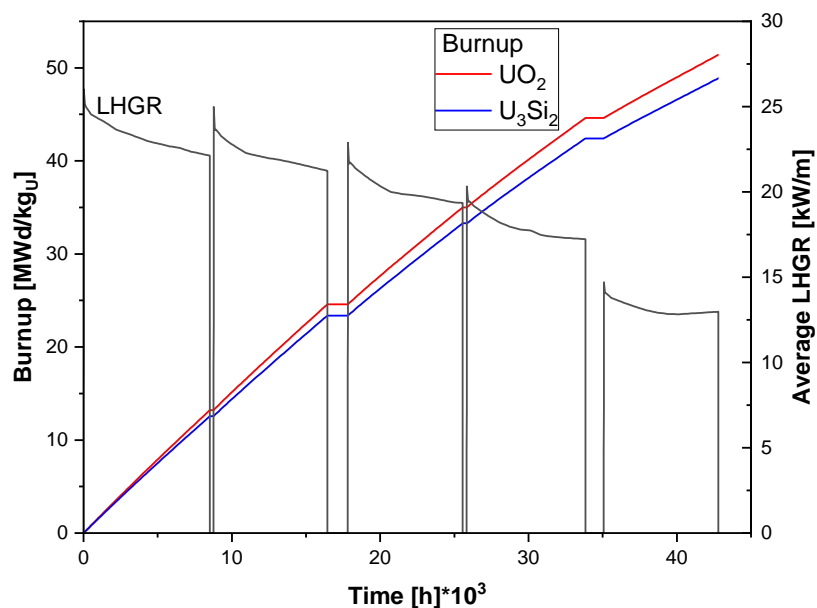


Figure 2: Calculated burnup. The LHGR history is plotted as a reminder.

## 4.1 Gap Closure

Since the same densification model is used for both fuel materials, the difference in calculated gap size is expected to be mainly due to the effect of pellet swelling, and the cladding creep. In order to illustrate this, the gap thickness at rod mid-height is plotted in Figure 3.

On one hand, the absence of a creep model for SiC cladding delays the gap closure. Gap closure is essential to allow for a high heat transfer between the coolant and the cladding. In this respect, experimental data on SiC composite are essential. Until the data on SiC composite creep are available, one should proceed with caution when interpreting the results. On the other hand, the higher swelling rate of  $U_3Si_2$  allows for the gap to close earlier.

Figure 3 shows that after 5 cycles the  $UO_2/SiC$  concept has not yet experienced gap closure. The  $U_3Si_2/SiC$  concept experiences a gap closure towards the end of the fourth cycle, which is far beyond the period at which gap closure is predicted for the reference  $UO_2/Zr$  system – the end of the first cycle.

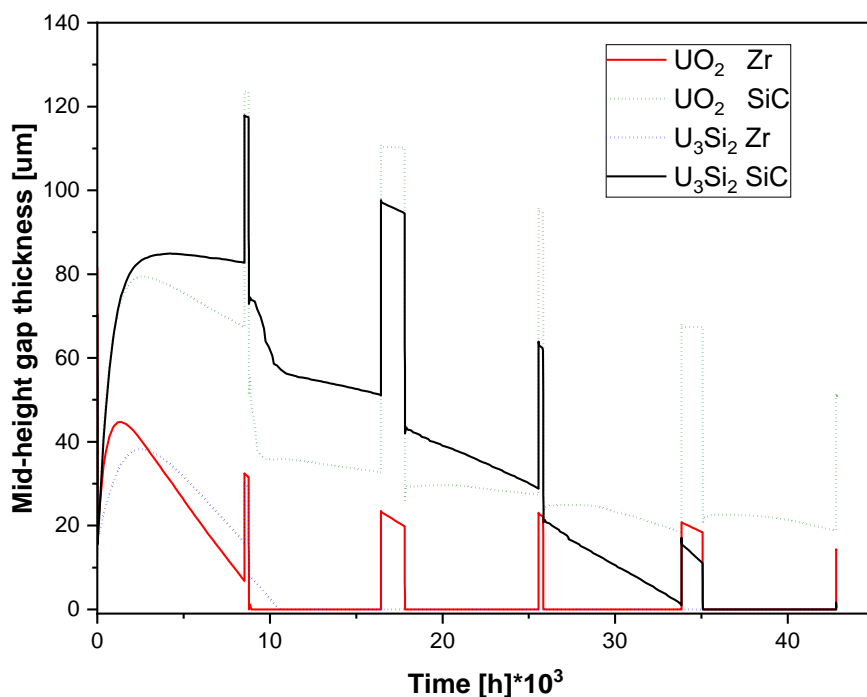


Figure 3: Gap thickness at rod mid-height.

## 4.2 Fuel/Cladding Temperature

The maximum temperature calculated for the fuel (centreline and outer surface) and cladding inner surface for each concept is shown in Figure 4. The cladding and fuel temperatures are the highest at the beginning of the second cycle, where the LHGR is high and the gap conductance is still low.

The fuel centreline temperature of the reference concept reaches a maximum value of 1600 K at this point. For the  $UO_2/SiC$  concept, the gap conductance is much higher and the fuel centreline temperature reaches 2400 K, approx. 600 K below the melting point of  $UO_2$ . The  $U_3Si_2$  concepts exhibit much lower temperatures. This is a direct consequence of the higher thermal conductivity of the ATF fuel material in question.  $U_3Si_2/SiC$  reaches a maximum fuel centreline temperature of 1350 K although the gap transfer is still low. This is also approx. 600 K below the melting point of the fuel. The maximum fuel outer surface temperatures are 1250 K and 1050 K for  $U_3Si_2/SiC$  and  $UO_2/Zr$ , respectively. The flattening of the temperature profile in the fuel due to the high thermal conductivity of the material can be seen in Figure 5. The low gap conductance for the  $UO_2/SiC$  concept at the end of irradiation can be deduced from the high temperature jump across the gap. Little difference can be observed for the maximal cladding temperature for the following reasons. Firstly, at the outer surface, the cladding is in

contact with the coolant and the cladding/coolant heat transfer is high. Secondly, the cladding wall thickness is small and, although the thermal conductivity can be low, the gradient of temperature in the cladding is limited.

These results indicate that the delayed gap closure and a low thermal conductivity of the cladding material are not critical from a thermal point of view in PWR operating conditions.

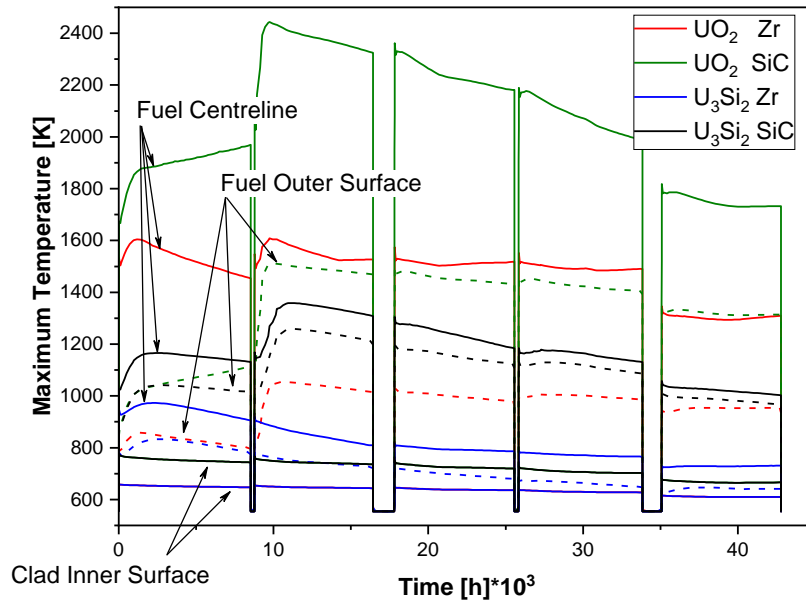


Figure 4: Maximal temperature calculated on the fuel centerline, fuel outer surface and clad inner surface for each fuel/cladding material concept.

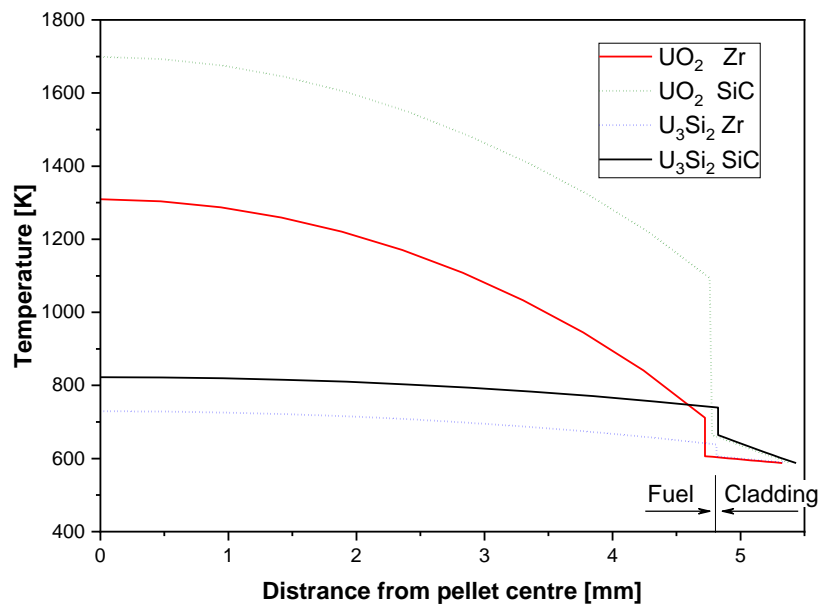


Figure 5: Temperature radial profiles calculated for each fuel/cladding concept.

### 4.3 Cladding Hoop Stress

The hoop (i.e. circumferential) stress at the inner element of the cladding is analysed here since this region is generally most critical for pellet-cladding interaction (PCI) in the presence of chemically aggressive fission products. The change from compressive to tensile stress (i.e. the

switch from negative to positive hoop stress) occurs shortly after the onset of pellet-cladding contact (or, after the pressure in the rod overcomes the pressure of the coolant – approx. 15.5 MPa). This change is predicted to occur in the beginning of the second cycle for the  $\text{UO}_2/\text{Zr}$  and the  $\text{UO}_2/\text{SiC}$  rods, in the middle of the second cycle for  $\text{U}_3\text{Si}_2/\text{Zr}$  and in the beginning of the last cycle for  $\text{U}_3\text{Si}_2/\text{SiC}$ . For the  $\text{UO}_2/\text{Zr}$ ,  $\text{UO}_2/\text{SiC}$  and  $\text{U}_3\text{Si}_2/\text{SiC}$  calculations, this change occurs upon gap closure, whereas for  $\text{UO}_2/\text{SiC}$ , only the gas pressure is exerted on the cladding inner surface.

The simulation shows that  $\text{U}_3\text{Si}_2/\text{SiC}$  undergoes a large hoop stress in the last cycle. A comparison with the Yield stress reported by Katoh [21] is possible since the strength from the SiC cladding stems from its composite layer. Therefore, the resulting hoop stress in the last cycle (approx. 128 MPa) might be too high and the gap closure might put the cladding integrity at risk. In this respect, it might be preferable that the gap closure does not take place with the  $\text{U}_3\text{Si}_2/\text{SiC}$  concept.

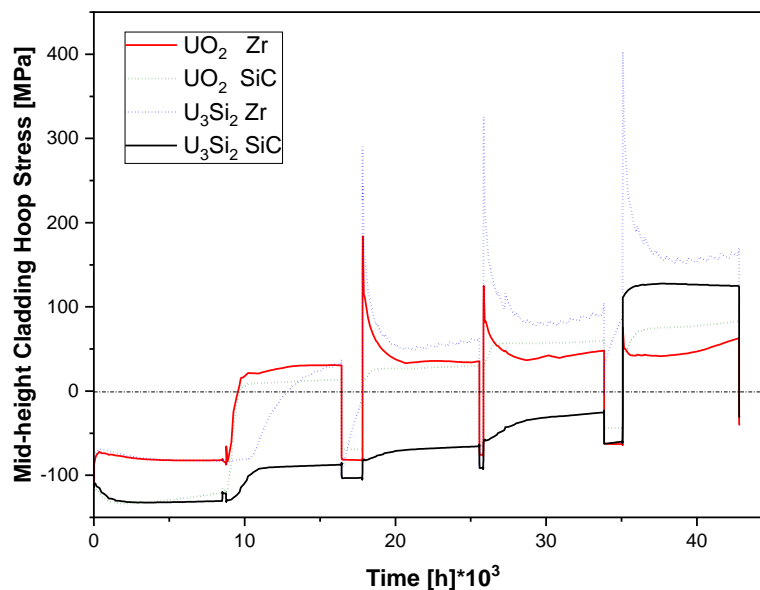


Figure 6: Hoop stress calculated for the cladding (inner surface) at mid-height.

## 5. Conclusions

Key properties of uranium silicide fuel and composite silicon carbide cladding have been integrated into the fuel performance code Falcon in order to conduct a scoping analysis on behaviour of an ATF rod under normal PWR operation conditions. The work has focused on the performance of  $\text{U}_3\text{Si}_2/\text{SiC}$  compared to the conventional  $\text{UO}_2/\text{Zr}$  system for a standard PWR irradiation history. The  $\text{UO}_2/\text{SiC}$  and  $\text{U}_3\text{Si}_2/\text{Zr}$  concepts were subject to the current intermediate analyses in order to help understand the impact of each material on the calculation results.

It has been presented that, in order to cope with a low thermal conductivity of SiC cladding, the high thermal conductivity of  $\text{U}_3\text{Si}_2$  is a clear advantage. Even though the melting point of  $\text{U}_3\text{Si}_2$  is lower than that of  $\text{UO}_2$ , the calculated fuel-cladding temperatures are reasonable. Considering low gap conductance and thermal conductivity of the cladding, the  $\text{U}_3\text{Si}_2/\text{SiC}$  concept still exhibits a fuel temperature much below the melting point. On the other hand, it was shown that the  $\text{U}_3\text{Si}_2/\text{SiC}$  concept undergoes high hoop stress upon gap closure with the current design. In order to reduce the hoop stress, one could delay the gap closure by increasing the cold gap thickness. The creep rate also has a direct impact on the gap closure. In order to address this point, it is critical to implement the creep rates of  $\text{U}_3\text{Si}_2$  and SiC. It is therefore considered a high priority to perform thermal and irradiation creep measurements on these materials in order to assess the performance of the  $\text{U}_3\text{Si}_2/\text{SiC}$  ATF concept.

To date, one of the most important issues seems to be a limited resistance of the SiC-based claddings to a failure due to pellet-cladding mechanical interactions (PCMI), particularly during

thermal transients. Advanced modelling might contribute into finding the optimal ATF-rod design and fuel properties, in combination with appropriate optimized irradiation conditions (see e.g. [22]). To this end, it is worthwhile considering development or extension of the advanced mechanistic models for fuel behaviour, such as e.g. the GRSW-A model coupled into FALCON [23], to candidate fuel materials, including predictive calculation of fuel densification, steady-state- and transient- swelling, fission gas release and other fuel related processes.

Although most key properties are already modelled in this Falcon version, the code is in continuous development and more conclusions will arise as more/better models related to these materials are used. Finally, it should be reminded that the current models reproduce behaviour of uranium silicide based on independent experiments; therefore a validation case (i.e. PIE on an actual rod) is required.

## Acknowledgments

The authors are thankful to swissnuclear for the financial support in the frame of the ATF project (LRT-02).

## References

- [1] S. Ray, S. G. Johnson, and E. Lahoda, "Preliminary Assessment of the Performance of SiC based Accident Tolerant Fuel in Commercial LWR systems," in *Proceedings of the 2013 Reactor Fuel Performance Meeting*, Charlotte, North Carolina, U.S.A., 2013.
- [2] K. Metzger, "Analysis Of Pellet Cladding Interaction And Creep Of U3Si2 Fuel For Us," U. of South Carolina, 2016.
- [3] D. S. Gomes, A. T. Silva, A. Y. Abe, R. O. R. Muniz, and C. Giovedi, "Simulation of accident-tolerant U3Si2 fuel using FRAPCON code," in *Proceedings of INAC 2017*.
- [4] S. Yagnik, "Falcon-Based Comparative Assessment of Prototype Zr-4 and SiC Fuel Rod," EPRI, Palo Alto, CA, USA, 1022907, 2011.
- [5] D. Carpenter, "Assessment of Silicon Carbide Cladding for High Performance Light Water Reactors," MSc. Thesis, Massachusetts Institute of Technology, 2007.
- [6] C. Cozzo *et al.*, "SiC Cladding Behaviour: Experiments and Modelling at PSI," in *Proceedings of the 2017 Water Reactor Fuel Performance Meeting*, Jeju, 2017.
- [7] R. J. White, S. B. Fisher, P. M. A. Cook, R. Stratton, C. T. Walker, and I. D. Palmer, "Measurement and analysis of fission gas release from BNFL's SBR MOX fuel," *J Nucl Mater*, vol. 288, pp. 43–56, 2001.
- [8] J. T. White, A. T. Nelson, J. T. Dunwoody, D. J. Safarik, and K. J. McClellan, "Corrigendum to 'Thermophysical properties of U3Si2 to 1773 K' [J. Nucl. Mater. 464 (2015) 275–280]," *J. Nucl. Mater.*, vol. 484, pp. 386–387, Feb. 2017.
- [9] A. Kaufmann, B. Cullity, and G. Bitsianes, "Uranium-Silicon Alloys," *J. Met.*, vol. 9, pp. 23–27, Jan. 1957.
- [10] J. Ahn, M. Lee, and S. Ahn, "UO2-based accident-tolerant hybrid fuel: a comparative study of high thermal conductivity additives," in *Proceedings of the WRFPM2017*, 2017.
- [11] P. Villars and K. Cenzual, *U3Si2 Crystal Structure: Datasheet from "PAULING FILE Multinaries Edition – 2012" in SpringerMaterials* ([https://materials.springer.com/isp/crystallographic/docs/sd\\_1922116](https://materials.springer.com/isp/crystallographic/docs/sd_1922116)). Springer-Verlag Berlin Heidelberg & Material Phases Data System (MPDS), Switzerland & National Institute for Materials Science (NIMS), Japan.
- [12] J. M. Harp, P. A. Lessing, and R. E. Hoggan, "Uranium Silicide Pellet Fabrication by Powder Metallurgy for Accident Tolerant Fuel Evaluation and Irradiation," INL, INL/JOU-15-34239.
- [13] U. Carvajal-Nunez, M. S. Elbakhshwan, N. A. Mara, J. T. White, and A. T. Nelson, "Mechanical Properties of Uranium Silicides by Nanoindentation and Finite Elements Modeling," *JOM*, vol. 70, no. 2, pp. 203–208, Feb. 2018.
- [14] K. M. Taylor and C. H. McMurtry, "Synthesis and Fabrication of Refractory Uranium Compounds. Summary Report for May 1959 Through December 1960," Carborundum Co. Research and Development Div., Niagara Falls, N.Y., ORO-400, Feb. 1961.
- [15] H. Shimizu, "The Properties and Irradiation Behavior of U3Si2," *Atomics International*, Canoga Park, Calif., NAA-SR-10621, Jul. 1965.
- [16] M. R. Finlay, G. L. Hofman, and J. L. Snelgrove, "Irradiation behaviour of uranium silicide compounds," *J. Nucl. Mater.*, vol. 325, no. 2, pp. 118–128, Feb. 2004.
- [17] G. L. Hofman, J. Rest, and J. L. Snelgrove, "Comparison of Irradiation Behavior of Different Uranium Silicide Dispersed Fuel Element Designs," ANL/RERTR/TM-18, 1997.



- [18] S. Yagnik, "Fuel Analysis and Licensing Code: FALCON MOD01, Volume 1: Theoretical and Numerical Bases," EPRI, Palo Alto, CA, USA, 1011307, 2004.
- [19] "BEMUSE Phase IV Report: simulation of a LB-LOCA in ZION Nuclear Power Plant," OECD/NEA, NEA/CSNI/R(2008)6/VOL2, 2008.
- [20] C. Cozzo and S. Rahman, "SiC cladding thermal conductivity requirements for normal operation and LOCA conditions," *Prog. Nucl. Energy*, vol. 106, pp. 278–283, Jul. 2018.
- [21] Y. Katoh, L. L. Snead, T. Nozawa, S. Kondo, and J. T. Busby, "Thermophysical and mechanical properties of near-stoichiometric fiber CVI SiC/SiC composites after neutron irradiation at elevated temperatures," *J. Nucl. Mater.*, vol. 403, no. 1, pp. 48–61, Aug. 2010.
- [22] G. Khvostov, "Technical note: On modelling central void formation in LWR fuel pellets due to high-temperature restructuring," *Nucl. Eng. Technol.*, Jul. 2018.
- [23] G. Khvostov, "A Dynamic Model for Fission Gas Release and Gaseous Swelling Integrated into the FALCON Fuel Analysis and Licensing Code," in *Proceedings of Top Fuel 2009*, Paris, France, 2009.